

## Cooperative bearing behaviors of roadside support and surrounding rocks along gob-side

Yunliang Tan<sup>1,2a</sup>, Qing Ma<sup>\*2</sup>, Zenghui Zhao<sup>1,2b</sup>, Qingheng Gu<sup>2c</sup>, Deyuan Fan<sup>2d</sup>, Shilin Song<sup>2e</sup> and Dongmei Huang<sup>1,2f</sup>

<sup>1</sup>State Key Laboratory of Mining Disaster Prevention and Control Co-founded by Shandong Province and the Ministry of Science and Technology, Qingdao 266590, China

<sup>2</sup>College of Mining and Safety Engineering, Shandong University of Science and Technology, Qingdao 266590, China

(Received November 17, 2018, Revised July 5, 2019, Accepted July 8, 2019)

**Abstract.** The bearing capacity of roadside support is the key problem in gob-side entry retaining technology. To study the cooperative bearing characteristics of the roof-roadside support-floor along the gob-side entry retaining, a mechanical model of the composite structure of the roof-roadside support-floor was first established. A method for determining the structural parameters of gob-side entry retaining was then proposed. Based on this model, adaptability analysis of roadside support was carried out. The results showed that the reasonable width of the gob-side entry roadway was inversely proportional to the mining height, and directly proportional to the bearing strength of the roof and floor. And the reasonable width of the “flexible-hard” roadside support was directly proportional to its own strength, and inversely proportional to the width of the gob-side entry retaining. When determining the position and size of the roadside support along the gob-side entry retaining, the surrounding rock environment should be fully considered. Measured results from case study also show the rationality of the model and calculation method.

**Keywords:** “flexible-hard” roadside support; composite structures; cooperative bearing capacity; gob-side entry retaining

### 1. Introduction

The technique of gob-side entry retaining could date back to the early 1950s. This technology can not only reduce the driving rate of roadways in mining areas, but also eliminate the replacement tension of the working face, reduce the cost of the retaining roadway, and prevent the underground disasters caused by the protection of coal pillar and coal lost. Simultaneously, Y-type ventilation can be realized, and explosion accidents caused by gas accumulation can also be prevented (Ning *et al.* 2018, Song *et al.* 2010, Ma *et al.* 2018, Mazaira *et al.* 2015, Cording *et al.* 2015). Therefore, this technique has been an important

focus in coal mining development.

The bearing capacity and type selection design of the roadside support is the main problem of gob-side entry retaining technology (Yang *et al.* 2016, Liu *et al.* 2018, Zhao *et al.* 2018, Yin *et al.* 2018). The fracture and rotary sinking of the lateral roof of the goaf is the main stress source of the roadside support body (Han *et al.* 2014). Although the roadway is located in a low stress area in the space after the mining, it cannot avoid the severe effect of the redistribution of the mining support stress. The mining pressure is strong and the roadway maintenance is difficult (Kaiser *et al.* 2012, Guo *et al.* 2018, Jiang *et al.* 2019). To this end, scholars have extensively researched the roadside support in the roadway. The existing results show that under the support of anchor and support, the roadway support has experienced the support system such as I-beam, U steel and so on, and has been developed to the present high strength bolt support system. It has basically been able to adapt to various surrounding rock deformation (Paul *et al.* 2012, Komurlu *et al.* 2016, Ivanovi *et al.* 2003, Ma *et al.* 2014). In addition to the traditional gangue stacking, wooden stacks, dense pillars and other traditional support methods, high-water material roadside support (Wang *et al.* 2018, Huang *et al.* 2018, Thompson *et al.* 2012) and paste material roadside support (Cui *et al.* 2016, Jiang *et al.* 2016, Wang *et al.* 2016, Pappas *et al.* 1993, Qi *et al.* 2018) have also been proposed. However, although the high water quick-setting material roadside support and paste material roadway support can achieve the effective use of underground gangue. The problem of high water fastening material is

\*Corresponding author, Ph.D. Student

E-mail: 1920687275@qq.com

<sup>a</sup>Professor

E-mail: yunliangtan@163.com

<sup>b</sup>Professor

E-mail: qzzh2004@163.com

<sup>c</sup>Ph.D. Student

E-mail: 1090047040@qq.com

<sup>d</sup>Ph.D. Student

E-mail: 2460791279@qq.com

<sup>e</sup>Ph.D. Student

E-mail: 617184810@qq.com

<sup>f</sup>Professor

E-mail: kmcandy@126.com

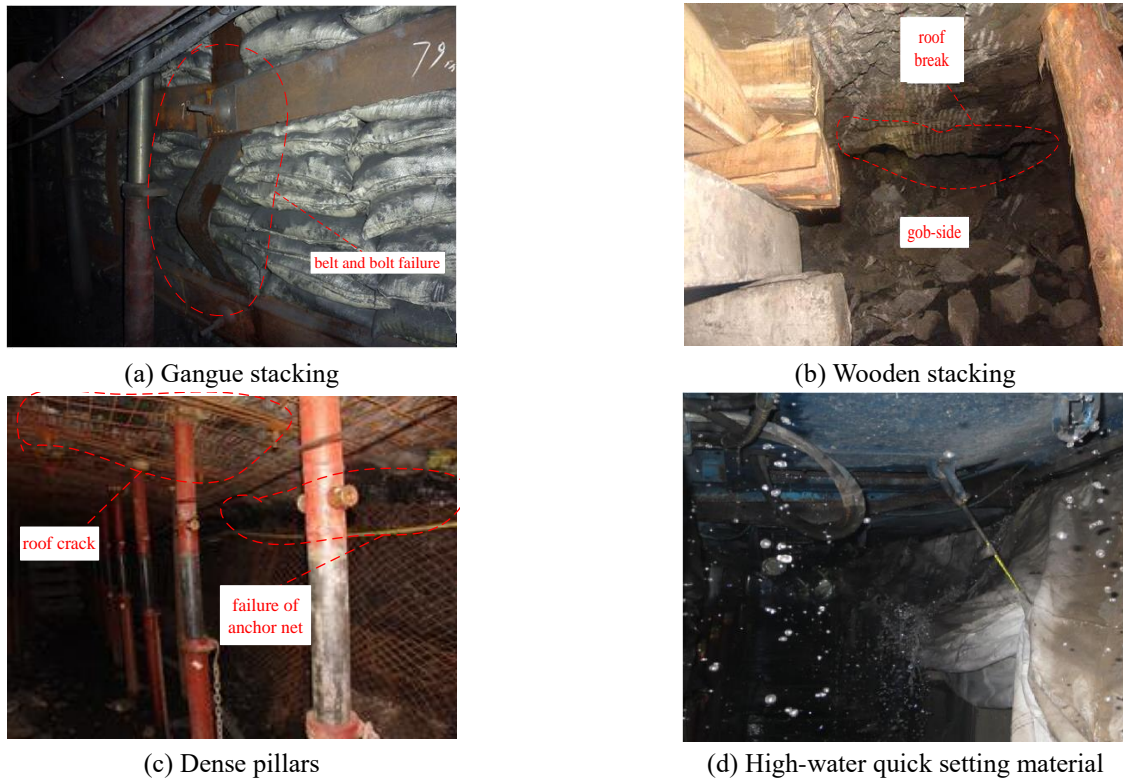


Fig. 1 Roadside support forms(Ma *et al.* 2018, Shi 2014)

more water consumption, large plastic deformation and high cost. Although the paste filling material has lower cost and significant economic benefits, the roadside support is easily crushed due to the small shrinkage. Therefore a “flexible-hard” combination of roadside support structure was proposed by Tan *et al.* (Tan *et al.* 2015, Fan *et al.* 2019). The flexible layer of the “flexible-hard” roadside support can avoid the instability of the support structure along the gob-side roadway and the occurrence of rockburst accidents caused by the dynamic pressure impact caused by the severe settlement movement of the roof rock beam. Ning *et al.* and Jiang *et al.* (Ning *et al.* 2014, Jiang *et al.* 2017) further applied this roadside support concept along gob-side entry retaining in deep coal mine, and obtained the mechanical properties curve of the roadside support and the reasonable working conditions.

The “flexible-hard” roadside support provides a new idea for retaining support technology along gob-side entry retaining. However, current research is mainly focused on the design, supporting mechanism, and deformation characteristics of the “flexible-hard” roadside support. There is limited research on the cooperative bearing capacity between roadside support and surrounding rocks. In fact, the load is passed through the rocks and the final load is shared by the support body and the rocks of the roof and floor. Thus, a composite bearing structure composed of the “roof-roadside support-floor” is formed. The environment of the surrounding rocks should be fully considered, and the location and size of the support should be rationally determined. It is often difficult to fully exert its bearing capacity by neglecting the conditions of occurrence and by simply increasing the strength and width of the roadside support, which is also not conducive to the

maintenance of roadway roof and floor. Therefore, the roadside support and surrounding rocks structure was considered as a composite structure in this study. Based on the bearing characteristics of the composite structure, the mechanical characteristics of composite structure cooperative bearing were established. Then a method for determining the strength and structural parameters of the support body was proposed and the adaptability of the roadside support was analyzed. Finally, the relevant theoretical methods were tested in engineering applications.

## 2. Bearing capacity of the composite structure

Apart from the traditional support methods, such as gangue stacking, wooden stacking, and dense pillars, roadside supports with a high-water quick-setting material and paste material have also proposed. However, there are various disadvantages of roadside support with these materials, such as failure of support, large deformation of the roadway, and possibility of other disasters. These roadside support forms are shown in Fig. 1.

The “flexible-hard” roadside support is a new approach in retaining technology along gob-side entry retaining. The bearing characteristics of roadside support and surrounding rocks are analyzed in the following text. The roof begins to sink along with the fracture of the rock beam in the middle of the goaf. Depending on whether the roof rock beam in the upper part of the coal seam breaks and contacts the gangue and the degree of compaction of the gangue, the bearing capacity of the composite structure of roadside support and surrounding rocks is divided into three periods, as shown in Fig. 2. The bearing structure of the roadside

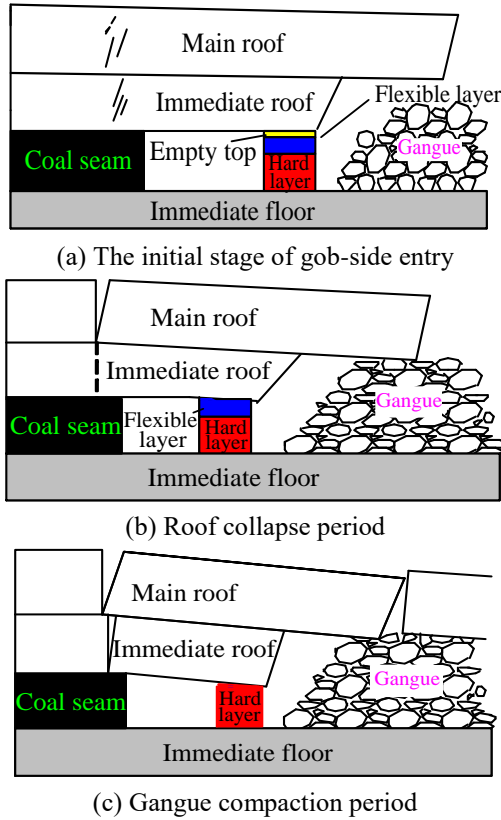


Fig. 2 Bearing characteristics of roadside support and surrounding rocks in different periods

support and surrounding rocks in different periods has the following bearing characteristics:

(1) The initial stage of gob-side entry retaining (Fig. 2(a)). At this stage, the upper part of the coal seam roof rock beam has not yet broken, but some small cracks have started to appear. The roof subsides slowly and gradually touches the backfill beside the roadway. However, because of the filling of the flexible material, the formation of the flexible layer is followed by the empty top phenomenon. Thus, the stage of the roadside support body does not play a supporting role on the roof, and the gob-side of the immediate roof is not exposed to the gangue. The weight of the roof is mainly borne by the coal and the immediate floor.

(2) Roof collapse period (Fig. 2(b)). At this stage, the upper part of the coal seam is broken, and the overlying strata undergoes rapid rotation subsidence. The empty top part of the roadside support body is compacted. The flexible layer of the roadside support plays a supporting role. The immediate roof contacts the gangue at the gob-side. The gangue in the goaf is in a state of compression and rheology. Therefore, at this stage, the weight of the roof is mainly shared by the coal, the roadside support body flexible layer, the immediate floor, and the gangue.

(3) Gangue compaction period (Fig. 2(c)). With the rapid rotation of the roof after the break down, the roadside support body's flexible layer and gangue are gradually compacted. The hard layer begins to play a supporting role. Thus, the sinking rate of the roof gradually reduces until the roof attains stability. The gangue is basically in the

compacted state. The acting force of the gangue on the roof is maximal. At this stage, the weight of the roof is shared by the coal, the hard layer of roadside support, and the compacted gangue.

### 3. Cooperative bearing behavior of the composite structure

#### 3.1 Mechanical model of gob-side entry retaining

Because of the large subsidence of the roof, the movement, deformation, and rupture of the support are easily caused (Fu *et al.* 2009). From the above analysis, the weight of the roof at different stages is shared by the coal, immediate floor, flexible-hard roadside support, or gangue. The mechanical model of the gob-side entry retaining is shown in Fig. 3. In the figure,  $L_1$  is the horizontal distance from the basic horizontal rotation of the base point to the coal side;  $L_2$  is roadway width;  $L_3$  is the width of the flexible-hard roadside support;  $L$  is the length of the main roof rock beam;  $h_b$ ,  $h_d$ ,  $h_m$ ,  $h_f$  are the thicknesses of the main roof, immediate roof, coal, immediate floor thickness, respectively;  $h_w$  and  $h_s$  are the heights of the flexible layer and the hard layer of flexible-hard roadside support, respectively.

#### 3.2 The bearing characteristics of the composite structure in the initial stage of gob-side entry retaining

In this stage, the bearing characteristics of the roadway support show that the weight of the roof is mainly

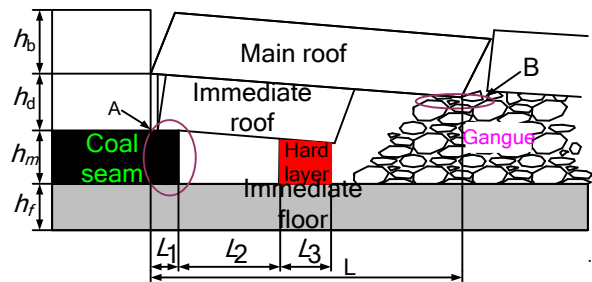


Fig. 3 Mechanical model of gob-side entry retaining

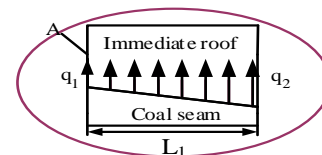


Fig. 4 Effect of coal on the roof in the initial stage of gob-side entry

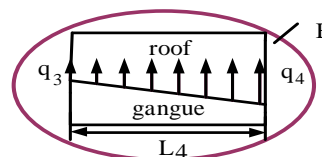


Fig. 5 The effect of gangue on roof in gangue compaction period

shared by the coal and the immediate floor. The effect of coal on the roof is simplified to a linear distribution, as shown in Fig. 4. Here,  $q_1$  and  $q_2$  are the load intensities at the rock beam and the coal support.

The force of solid coal on the roof is  $F_M$

$$F_M = \frac{1}{2} L_1 (q_1 + q_2) \quad (1)$$

### 3.3 The bearing characteristics of the composite structure in the roof collapse period

In the early stage of roof movement, the compression of the flexible layer is better. It can relieve the subsidence of the roof, release the impact pressure on the roof, and prevent the impact of the dynamic pressure or rock burst. It can also lower the roadway support resistance and prevent crushing of the support body. In the process of bending and subsidence of the roof rock beam, the coal block has been acting until the main roof begins to touch the gangue. The force is still  $F_M$ . Suppose that the force of the gangue on the roof is linear, as shown in Fig. 5. The load intensity at the left and right sides of the roof touching the gangue is  $q_3$  and  $q_4$ , respectively.

From Fig. 5, the size of gangue force in the goaf can be obtained

$$F_G = \frac{1}{2} (q_3 + q_4) L_4 \quad (2)$$

When the flexible layer is filled with the soft material, an unsupported roof is formed.  $\delta$  represents the empty top height. This part of the top of the roof during the slow sinking process will not contribute to the formation of the rock. With the slow sinking of the roof, the flexible layer of the support first plays a supporting role. The flexible layer force acting on the side support body is  $F_W$ .

$$F_W = E_W \Delta h_1 L_3 \quad (3)$$

where  $E_W$  is the supporting force of the unit length of the flexible layer support body compression unit length.  $\Delta h_1$  is the compression of the flexible layer of the support body.

### 3.4 The bearing characteristics of composite structure in the gangue compaction period

At the end of the roof movement, as the roof of the rotation subsides, the support of the flexible layer is compacted, and the hard layer begins to play the support role. The hard layer can better support the overlying roof's weight. At this stage, the impact of the coal on the roof will change. The acting force of the coal is assumed to be  $F'_C$ . The gangue in the goaf is in a compressed rheological state. As the gangue is gradually compacted, the weight of the roof is shared by the coal, gangue, and hard layer of the support body. The forces of the support body's hard layer and the gangue on the roof are  $F_S$  and  $F'_G$ , respectively. As the gangue is gradually compressed, the equivalent coefficient of expansion decreases. The relationship

between the rheological strain and the coefficient of expansion of the gangue can be expressed by the following equation (Yang *et al.* 2015, Guo *et al.* 2016).

$$\varepsilon = \frac{K_a - K_t}{K_a} \quad (4)$$

where  $K_a$  is the immediate roof expansion coefficient,  $K_t$  is the equivalent coefficient of expansion of immediate roof at time  $t$ .

It is assumed that the area of the gangue to the roof is  $A_g$ . The elastic modulus of the gangue is  $E_g$ . The force of the gangue on the roof  $F'_G$  is expressed as follows

$$F'_G = E_g \varepsilon A_g \quad (5)$$

Substituting Eq. (2) into Eq. (3)

$$F'_G = E_g A_g \frac{(K_a - K_t)}{K_a} \quad (6)$$

The weights of the immediate roof and the main roof are  $M_d$  and  $M_b$ , respectively

$$M_d = \gamma_d h_d (L_1 + L_2 + L_3) \quad (7)$$

$$M_b = \gamma_b h_b L \quad (8)$$

where  $\gamma_d$  is the immediate roof bulk density, and  $\gamma_b$  is the main roof bulk density.

It is assumed that the fault line of the roof slab in the coal runs through the immediate roof and the main roof rock beam. The entire support structure can be seen from the mechanical equilibrium conditions.

$$\begin{cases} \sum F = 0 \\ \sum M = 0 \end{cases}$$

$F'_C$  and  $F_S$  can be deduced as follows

$$F'_C = \frac{\gamma_d h_d A^2 + \gamma_b h_b L B - \frac{2E_g A_g (K_a - K_t)}{K_a} C}{D} \quad (9)$$

$$F_S = \frac{\gamma_d h_d A (L_2 + L_3) + \gamma_b h_b L (L - L_1) - \frac{E_g A_g (K_a - K_t)}{K_a} (2L - L_1)}{D}$$

where

$$A = L_1 + L_2 + L_3, B = 2L_1 + 2L_2 + 2L_3 - L$$

$$C = L - L_1 - L_2 - L_3, D = L_1 + 2L_2 + 2L_3$$

## 4. Bearing capacity and structural characteristics of composite structure

### 4.1 Strength parameter of roadside support body

The roof load is first analyzed. The weight of the overlying strata is assumed by the retaining coal and the "flexible-hard" support before the initial contact with the

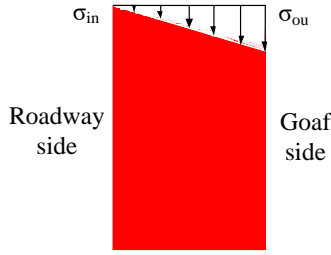


Fig. 6 The inner stress and outer stress of the roadside support body

gange. According to the theory of mining strata (Liu *et al.* 2016),

$$\sigma_1 = \frac{(L_1 + L_2 + L_3)h_d\gamma_d + Lh_b\gamma_b - F_c}{L_3} \quad (10)$$

The strength development of the “flexible-hard” support body takes some time. Eq. (10) applies to the initial stage of gob-side entry retaining before the main roof rupture. Therefore, it should be calculated based on the initial strength.

Then consider the basic load at the end of the gob-side entry. Until the full contact of the gange, the different positions of the roof set the amount of deformation  $S_x$ .

$$S_x = \frac{2\Delta h x}{c_0} \quad (11)$$

where,  $c_0 = \sqrt{2h_1[\sigma_{t2}]/\gamma_d}$ ,  $\Delta h = h_m + h_d - K_a h_d$ ,  $x$  is the horizontal distance from the main roof break point,  $c_0$  is the initial weighting interval, and  $\sigma_{t2}$  is the allowable tensile stress of the immediate roof.

By using Eq. (4), the amount of compression deformation of the gange can be obtained

$$\Delta h_g = \frac{(K_a - K_t)(h_m + h_d)}{K_a} \quad (12)$$

$\sigma_x$  is used to indicate the compressive stress of the lower rock mass from the main roof breaking point at different horizontal distances. The main roof of the lower rock mass compression deformation  $\Delta h_x$  is

$$\Delta h_x = \frac{\sigma_x h_d}{E_d} + 3\frac{\sigma_x h_f}{E_f} + \frac{\sigma_x h_w}{E_w} + \frac{\sigma_x h_s}{E_s} + \frac{(K_a - K_t)(h_m + h_d)}{K_a} + \delta \quad (13)$$

where,  $E_d$ ,  $E_f$ ,  $E_w$ , and  $E_s$  are the elastic modulus of the immediate roof, immediate floor, flexible layer of the “flexible-hard” support, and hard layer of the “flexible-hard” support respectively.

Because the lower rock mass is in a given deformation state,  $S_x = \Delta h_x$ .  $\sigma_x$  can be obtained by solving the simultaneous formula of Eq. (11) and Eq. (13).

$$\sigma_x = \frac{2K_a [h_m - (K_a - 1)h_d]x - c_0\delta K_a - c_0(K_a - K_t)(h_m + h_d)}{c_0 K_a \left( \frac{h_d}{E_d} + 3\frac{h_f}{E_f} + \frac{h_w}{E_w} + \frac{h_s}{E_s} \right)} \quad (14)$$

Under the existing technical conditions, the strength of

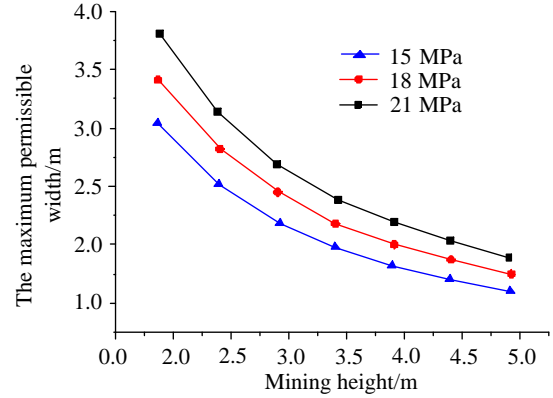


Fig. 7 The maximum permissible gob-side entry retaining width with the change of mining height

the support can easily meet the requirements of Eq. (10). However, the Eq. (14) shows that the latter requires higher strength. Thus,  $\sigma_x$  is proportional to  $x$ . The pressure of the “flexible-hard” support body can be relieved by reducing the width of the support and the roadway.  $\sigma_x$  is inversely proportional to  $c_0$ . The value of  $c_0$  can be increased by increasing the thickness and intensity of the immediate roof. This can reduce the force of the “flexible-hard” support body.

## 4.2 Structure parameters of gob-side entry retaining and support body

### 4.2.1 Reasonable width of the gob-side entry retaining

The inner stress  $\sigma_{in}$  and outer stress  $\sigma_{ou}$  of the roadside support body are shown in Fig. 6.

The stress  $\sigma_{in}$  on the inside of the roadside support is obtained from Eq. (14)

$$\sigma_{in} = \frac{2K_a [h_m - (K_a - 1)h_d](L_1 + L_2) - c_0\delta K_a - c_0(K_a - K_t)(h_m + h_d)}{c_0 K_a \left( \frac{h_d}{E_d} + 3\frac{h_f}{E_f} + \frac{h_w}{E_w} + \frac{h_s}{E_s} \right)} \quad (15)$$

When the strength of the roof and floor is lower than the stress inside the support, the rock stratum will be cut. Thus, the roof stress inside the support body should be smaller than the smallest strength of the immediate roof and immediate floor, which is given as

$$\sigma_{in} \leq R_m = \min(R_r, R_f) \quad (16)$$

By combining with Eq. (15) and Eq. (16), the upper limit the width of the gob-side entry retaining can be obtained.

$$L_2 \leq \frac{\left[ R_m K_a \left( \frac{h_d}{E_d} + 3\frac{h_f}{E_f} + \frac{h_w}{E_w} + \frac{h_s}{E_s} \right) + K_a\delta + (K_a - K_t)(h_m + h_d) \right] c_0}{2K_a [h_m - (K_a - 1)h_d]} \cdot L_1 \quad (17)$$

As for the width of roadway, the lower limit can be determined according to the demand of the section in production. The allowance of deformation should be considered in the design. This is not discussed here.

The minimum strength  $R_m$  of the immediate roof and the

immediate floor mass is 15, 18 and 21 MPa respectively. The thickness of immediate roof  $h_d$  is 3.4 m. The remaining parameters are consistent with the former. When the mining height is increased from 2 m to 5 m, the maximum of permitted gob-side entry retaining roadway's width can be obtained by Eq. (17). As shown in Fig. 7, the following conclusions can be drawn: (1) The maximum permissible gob-side entry retaining width is inversely proportional to the mining height; (2) The maximum permissible gob-side entry retaining width increases with the increase of  $R_m$ . By reducing the height of the mining or increasing the bearing strength of the immediate roof and immediate floor, the width of the gob-side entry retaining is increased.

4.2.2 Reasonable width of "flexible-hard" roadside support

The lower limit of the width of the "flexible-hard" roadside support can be obtained from Eq. (10).

$$L_3 \geq \frac{(L_1 + L_2)h_d\gamma_d + Lh_b\gamma_b - F_C}{\sigma_1 - h_d\gamma_d} \tag{18}$$

The roadside "flexible-hard" support body's lateral stress can be obtained from Eq. (14).

$$\sigma_{ou} = \frac{2K_a[h_m - (K_a - 1)h_d](L_1 + L_2 + L_3) - c_0\delta K_a - c_0(K_a - K_i)(h_m + h_d)}{c_0K_a\left(\frac{h_d}{E_d} + 3\frac{h_f}{E_f} + \frac{h_w}{E_w} + \frac{h_s}{E_s}\right)} \tag{19}$$

When the lateral stress is higher than the support strength, the support will be fractured. Therefore, the stress on the outer side of the flexible-hard support body cannot be greater than the support strength  $R_b$ , which is given as

$$\sigma_{ou} < R_b \tag{20}$$

The upper limit of the width of the "flexible-hard" support body with the strength  $R_b$  can be obtained by combining Eq. (19) and Eq. (20).

$$L_3 \leq \frac{\left[R_b\left(\frac{h_d}{E_d} + 3\frac{h_f}{E_f} + \frac{h_w}{E_w} + \frac{h_s}{E_s}\right) + \delta K_a + (K_a - K_i)(h_m + h_d)\right]c_0}{2K_a[h_m - (K_a - 1)h_d]} \cdot (L_1 + L_2) \tag{21}$$

(1) From Eq. (18), it can be seen that the lower limit of the width of the "flexible-hard" support is related to the width of the coal-bearing strands  $L_1$ , the lane width  $L_2$ , and the immediate roof and main roof thicknesses  $h_d$  and  $h_b$ ; From Eq. (21), we can see that the upper limit of the "flexible-hard" support is related to its own strength  $R_b$ , the roadway size and the initial pressure step  $C_0$ . The immediate roof thickness  $h_d$ , lane width  $L_2$  and initial pressure step  $C_0$  are 3.0m, 2.5m and 30.0m respectively. The strength  $R_b$  of "flexible-hard" support is 3, 6 and 9MPa respectively. The flexible layer of the "flexible-hard" support plays a supporting role in the early period. The initial strength  $\sigma_1$  is 1/10 of the intensity  $R_b$ . The remaining parameters are consistent with the former. The upper and lower limits of the support width are obtained under the influence of its own strength, as shown in Fig. 8.

From Fig. 8, we can draw the following conclusions. (a) The upper limit of the width of the support is proportional to its own strength; (b) The allowable width of the support

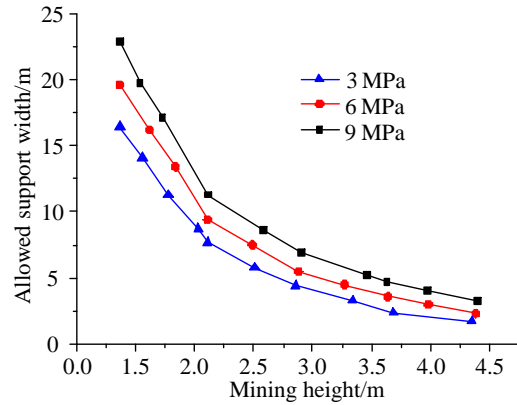


Fig. 8 The allowed support width with the change of its strength

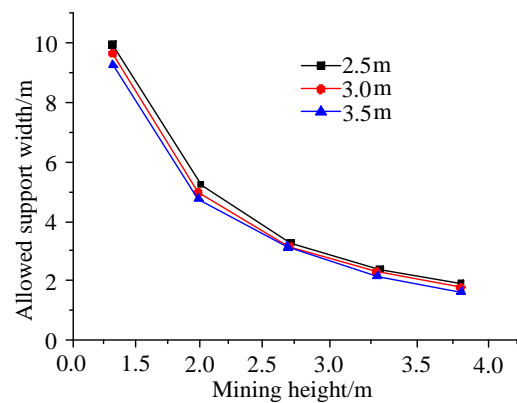
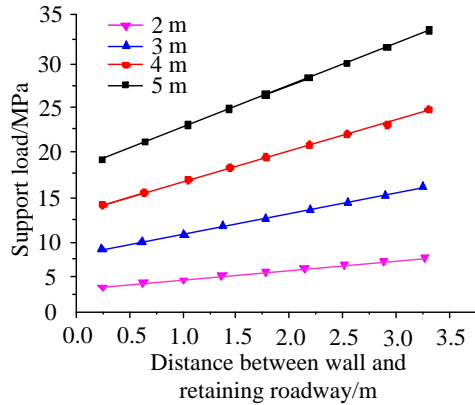


Fig. 9 The allowed support width with the change of gob-side entry retaining width

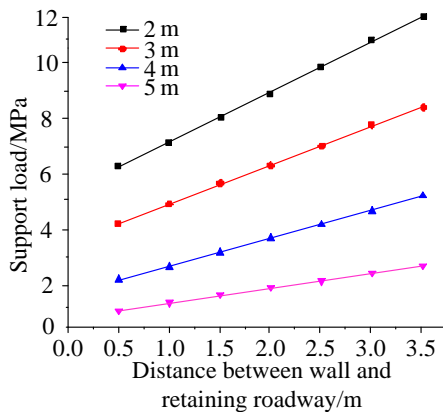
decreases with increasing height, but the range of reduction also decreases. These indicate that the support must bear a higher roof pressure when the mining height is increased. Thus it is necessary to increase the width of the support. Simultaneously, the increase in the height increases the given deformation. When the support width is too large, it will be damaged due to excessive given deformation. Thus, the width of the support should be reasonable in the upper and lower limits; The flexible layer has a larger shrinkage in the early movement of roof strata. In the case of maintaining the support body itself is not damaged, allowing the roof to produce a certain sink; In the late stage of the roof rock movement, the hard layer of support body has a high support resistance. The hard layer supports the roof weight and breaks the roof.

(2) The strength of support body  $R_b$  is 3MPa. The remaining parameters are consistent with the former. The upper limit of the width of the support is affected by the width of the roadway as shown in Fig. 9. As can be seen from the figure, the upper limit of the width of the support is inversely proportional to the roadway width.

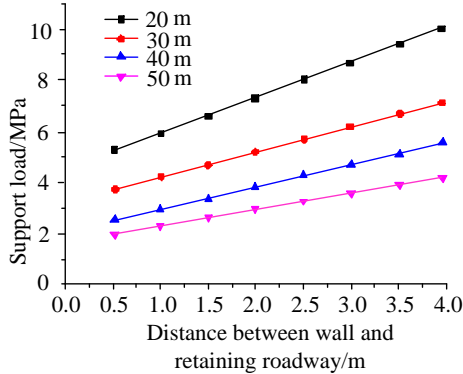
Under certain roof conditions, the width of the support depends on the initial and final strengths of the support, the mining height, and the roadway width. These parameters determine the upper and lower limits of the support width. The width of support body can be reduced mainly by reducing the mining height, improving the initial strength



(a) The change of support load with mining height



(b) Support load changes with the thickness of the immediate roof



(c) The change of support load with initial weighting interval

Fig. 10 Support load curve

and reducing the span of the roadway.

#### 4.3 Adaptability analysis of roadside support

The influence of height and immediate on the bearing load can be analyzed by using Eq. (14). Take  $L_1$  as 3.0m,  $L$  as 20.0 m, and  $L_2$  as 2.5 m. The modulus of flexible layer and hard layer of “flexible-hard” support were  $E_W=100$  MPa,  $E_S=300$  MPa. The modulus of immediate roof and floor is  $E_d = E_f=200$  MPa.  $K_d=1.3$ . Empty top distance  $\delta=0.1$  m. The height of flexible layer is  $h_W=0.3$  m. The height of hard layer is  $h_s=1.6$  m.

(1) When the immediate roof thickness is  $h_d=3.4$  m and

the immediate floor is  $h_f=2$  m. The initial weighting interval is  $C_0=40.0$  m. And the height is increased from 2 m to 5 m, the load curve of the support is shown in Fig. 10(a). The bearing characteristics are as follows: (a) The side support load of roadway is less than that of gob-side. (b) The relationship between support load and mining height is proportional. The load of the support increases with increasing mining height. Obviously, when the height increases to a certain extent, the “flexible-hard” support body is crushed. Finally, it will lead to failure of gob-side entry retaining.

(2) When the mining height is 2 m and the immediate roof thickness  $h_d$  is increased from 2 m to 5 m, the bearing curve of the support is shown in Fig. 10(b). The support load is inversely proportional to the immediate roof thickness. The support load decreases as the immediate roof thickness increases. However, the range of reduction also decreases. The immediate roof can act as a buffer to the carrying capacity of the support. The thicker immediate roof is good for gob-side entry retaining.

(3) When the mining height is 2 m, the thickness of the immediate roof  $h_d$  is 3.4 m, and the initial weighting interval is increased from 20 m to 50 m. The load curve of the support is shown in Fig. 10(c). The support load is inversely proportional to the initial weighting interval. The support load decreases as the initial weighting interval increases. Therefore, the support load can be reduced by increasing the initial weighting interval. It can be seen from Eq. (11) that the initial weighting interval is proportional to the thickness of the immediate roof and its allowable tensile stress. Therefore, the immediate roof plays a key role in the success of the gob-side entry retaining.

## 5. Case study

### 5.1 Geological survey

11508 face of a mining company’s mining coal seam is 15. The thickness, average dip angle, and depth of the coal seam is 1.7 m,  $17^\circ$ , and 550 m, respectively. The immediate roof is made of mudstone with an average thickness of 4.4 m and strength of 18 MPa. The main roof has an average thickness of 8.4 m and is made of sandstone. The immediate floor is 2.55-m-thick and made of mudstone. Its strength is 20 MPa. The 11508 roadway section shape is trapezoidal. Its net width is 3.4 m and medium height is 2.5 m. The anchor bolt adopts the full-strength bolt with a diameter of 20 mm and the length of 2000 mm. The roof is anchored by two groups of anchor bolts to the two sides. The vertical angle to the roof plate is  $20^\circ$ - $30^\circ$ . The distance between the anchor bolts and the adjacent supports should be no less than 0.5 m. The distance between the two bolts of the roadway from the roof is not more than 400 mm. The inclination angle is adjusted according to the inclination of the roof in order to ensure that the anchorage section is in the roof rock. The two rows of bolts in the roadway are less than 600 mm from the roadway floor to the roof. The angle between the anchor and the horizontal axis is  $40^\circ$ - $50^\circ$ . The anchor section is located in the floor rock.

### 5.2 Design of roadside support

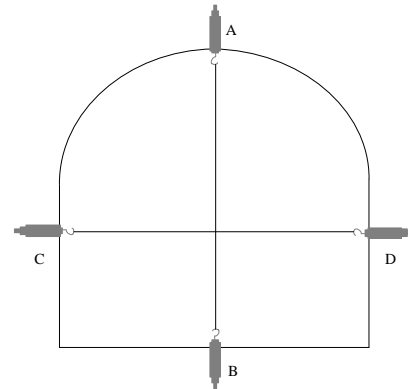
The basic parameters of the working face are obtained

Table 1 Calculation of bearing strength of roadside support body

Filling width/m	Required strength of filling material/MPa	Test strength(1d)/MPa
1.5	1.564	1.54
2.0	1.173	
2.5	0.938	
3.0	0.782	

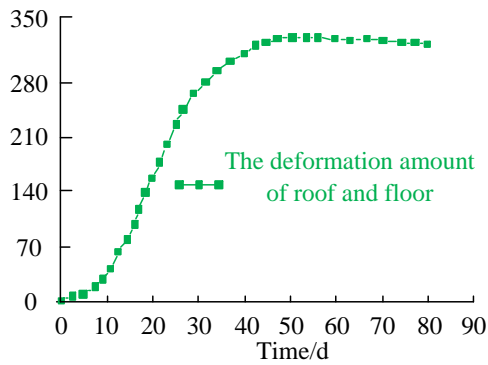


(a) Digital convergence apparatus

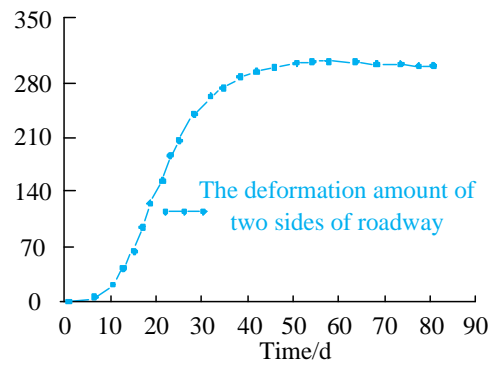


(b) Installation schematic diagram

Fig. 11 Digital convergence apparatus and its installation schematic diagram



(a)



(b)

Fig. 12 Field monitoring curve



Fig. 13 The effect of “flexible-hard” roadside support

by analyzing the distribution, structural and mechanical parameters, engineering experience, and monitoring results of similar working faces. The immediate roof thickness is  $h_d=4.4$  m. The bulk density is  $\gamma_d=25$  KN/m<sup>3</sup>. The main roof thickness is  $h_b=8.4$  m. The bulk density is  $\gamma_b=20$  KN/m<sup>3</sup>. The length of roof rock beam  $L=20$  m. The distance

between fracture line of the roof rock beam and the coal support is  $L_1=3.0$  m. The width of side support body is  $L_3=2.0$  m. The mining height is  $h_m=2.1$  m. The immediate roof rock’s expansion coefficient is  $K_a=1.3$ . The equivalent coefficient of expansion is  $K_r=1.1$  when the gangue is rheological and hardened. The compression length of the gangue in the goaf is 10 m. The coal support roof subsidence is  $\Delta h_0$ . The filling amount of the roadside support body is  $\Delta h_1$ .  $\Delta h$  is the maximum amount of subsidence for the main roof. The following conclusions can be drawn according to the covariance of deflection.

The collapse of the immediate roof rock will fill the gob-side entry retaining. The maximum allowed subsidence of the main roof is  $\Delta h$ .

Thus, when the main roof rock beam is bent to just touch the gangue, the height  $h_w$  of the flexible filling material is  $h_w \approx 0.33$  m. The height  $h_w$  of the soft filling material is 0.33 m. The height of the high-strength filling material  $h_s=h_m-h_w-\delta=1.67$  m. From Eq. (18) and Eq. (21), the roadway support body width range of  $1.21 \leq L_3 \leq 7.35$  can

be obtained.

In order to obtain a reasonable width of the support body, reference (Pappas *et al.* 1993, Recio-Gordo *et al.* 2012, Liu *et al.* 2019, Tan *et al.* 2019, Lyu *et al.* 2019, Schumacher and Kim 2014). According to Eq. (15), when the width of the support body is 1.5 m, 2.0 m, 2.5 m, 3.0 m, the bearing strength of the support body is shown in Table 1.

Table 1 shows that when the existing high-strength material is used to form the filling support, the width needs to be 2.0 m.

### 5.3 Field measurement of application effect

The 15 coal roadway support scheme is designed as follows: The flexible layer adopts height 0.33 m foam material. The hard layer uses concrete and has a height of 1.67 m. The width of the filling support is 2.0 m. Field observations indicate that the upper soft material has low strength and is basically compacted. The flexible layer prevents the rapid sinking of the roof. And it achieves an early pressure yield on the roof. The lower filling material has higher strength. It can achieve the burden of immediate load. The deformation of the two sides of roadway and the roof and floor is monitored by the digital convergence apparatus, as shown in Fig. 11. And the field monitoring curve is shown in Fig. 12. As can be seen from Fig. 12, the maximum deformation of the two sides of roadway and the maximum deformation of the roof and floor were 320.6 mm, 285 mm respectively. The amount of deformation meets the requirements of safe use of roadways. The effect of support is shown in Fig. 13.

## 5. Conclusions

Based on whether the roof rock beam is broken and the compaction degree of the gangue in the goaf, the bearing capacity of the composite structure of roadside support and surrounding rocks is divided into three periods: the initial stage of gob-side entry retaining, the roof collapse period, and the gangue compaction period. The weight of the roof rock in different periods will be supported by the coal, the roadside support, the gangue and the rocks of the roof and floor.

The strength of the “flexible-hard” roadside support is proportional to the width of the retaining roadway and the width of the roadside support body, and it is inversely proportional to the initial weighting interval. The maximum allowable roadway width along the gob-side entry retaining is inversely proportional to the mining height, and it is directly proportional to the minimum intensity of the immediate roof and the immediate floor. The upper limit of the width of the support is proportional to its own strength, and inversely proportional to the roadway width. The allowable width of the support decreases with increasing height, however, the range of reduction also decreases.

The load is transmitted through the rock formation and is ultimately supported by the composite structure. The surrounding rock environment where the roadside support is located should be fully considered. The location and size of

the roadside support should be reasonably determined. It is difficult to give full play to the bearing capacity when the strength and width of the support are neglected. This is also not conducive to the maintenance of roadway roof and floor.

According to the field application tests, when the support body of the roadway along the gob-side entry adopts the “flexible-hard” support body, the deformation of the roadway meets the safe use requirements of the roadway. It can effectively ensure the stability of the roadway along the gob-side entry retaining. However, more case studies are needed to study the effects of different buried depths, dynamic loading, machinery as well as rate of extraction on the “flexible-hard” roadside support along the gob-side entry retaining.

## Acknowledgments

The research described in this paper was financially supported by National Key R&D Program of China (Grant No. 2018YFC0604703), the National Natural Science Foundation of China (No. 51774196, Grant No. 51804181, No. 51874190), Major Program of Shandong Province Natural Science Foundation (ZR2018ZA0603), Shandong Province Natural Science Fund (no. ZR2018QEE002) and China Postdoctoral Science Foundation (No. 2016M592221).

## References

- Cording, E.J., Hashash, Y.M.A. and Oh, J. (2015), “Analysis of pillar stability of mined gas storage caverns in shale formations”, *Eng. Geol.*, **184**, 71-80. <https://doi.org/10.1016/j.enggeo.2014.11.001>.
- Cui, L. and Fall, M. (2016), “An evolutive elasto-plastic model for cemented paste backfill”, *Comput. Geotech.*, **71**, 19-29. <https://doi.org/10.1016/j.compgeo.2015.08.013>.
- Fan, D.Y., Liu, X.S., Tan, Y.L., Song, S.L., Gu, Q.H., Yan, L. and Xu, Q. (2019), “Roof cutting parameters design for gob-side entry in deep coal mine: A case study”, *Energies*, **12**, 2032. <https://doi.org/10.3390/en12102032>.
- Fu, Y.P., Song, X.M., Xing, P.W., Yan, G.C. and Li, Z.J. (2009), “Stability analysis on main roof key blocks in large mining height workface”, *J. Chin. Coal Soc.*, **34**(8), 1027-1031.
- Guo, W.Y., Tan, Y.L., Yu, F.H., Zhao, T.B., Hu, S.C., Huang, D.M. and Qin, Z.W. (2018), “Mechanical behavior of rock-coal-rock specimens with different coal thicknesses”, *Geomech. Eng.*, **15**(4), 1017-1027. <https://doi.org/10.12989/gae.2018.15.4.1017>.
- Guo, W.Y., Tan, Y.L., Zhao, T.B., Liu, X.M., Gu, Q.H. and Hu, S.C. (2016), “Compression creep characteristics and creep model establishment of Gangue”, *Geotech. Geol. Eng.*, **34**(4), 1193-1198. <https://doi.org/10.1007/s10706-016-0038-2>.
- Han, C.L., Zhang, N., Li, G.C., Li, B.Y. and Wu, H. (2014), “Stability analysis of compound bearing structure of gob-side entry retaining with large mining height”, *Chin. J. Geotech. Eng.*, **36**(5), 969-976.
- Ivanović, A., Starkey, A., Neilson, R.D. and Rodger, A.A. (2003), “The influence of load on the frequency response of rock bolt anchorage”, *Adv. Eng. Softw.*, **34**(11-12), 697-705. [https://doi.org/10.1016/S0965-9978\(03\)00099-1](https://doi.org/10.1016/S0965-9978(03)00099-1).
- Jiang, B.Y., Gu, S.T., Wang, L.G., Zhang, G.C. and Li, W.S. (2019), “Strainburst process of marble in tunnel-excavation-

- induced stress path considering intermediate principal stress”, *J. Central South Univ.*, **26**(4), 984-999. <https://doi.org/10.1007/s11771-019-4065-z>.
- Jiang, H., Mamadou, F. and Liang, C. (2016), “Yield stress of cemented paste backfill in sub-zero environments: Experimental results”, *Min. Eng.*, **92**, 141-150. <https://doi.org/10.1016/j.mineng.2016.03.014>.
- Jiang, L., Zhang, P., Chen, L., Hao, Z., Sainoki, A., Mitri, H.S. and Wang, Q. (2017), “Numerical approach for goaf-side entry layout and yield pillar design in fractured ground conditions”, *Rock Mech. Rock Eng.*, **50**(4), 1-23. <https://doi.org/10.1007/s00603-017-1277-0>.
- Kaiser, P.K. and Cai, M. (2012), “Design of rock support system under rockburst condition”, *J. Rock Mech. Geotech. Eng.*, **4**(3), 215-227. <https://doi.org/10.3724/SP.J.1235.2012.00215>.
- Komurlu, E., Kesimal, A. and Demir, S. (2016), “Experimental and numerical study on determination of indirect (splitting) tensile strength of rocks under various load apparatus”, *Can. Geotech. J.*, **53**(2), 545-564. <https://doi.org/10.1139/cgj-2014-0356>.
- Liu, X.S., Gu, Q.H., Tan, Y.L., Ning, J.G. and Jia, Z.C. (2019), “Mechanical characteristics and failure prediction of cement mortar with a sandwich structure”, *Minerals*, **9**(3), 143. <https://doi.org/10.3390/min9030143>.
- Liu, X.S., Ning, J.G., Tan, Y.L. and Gu, Q.H. (2016), “Damage constitutive model based on energy dissipation for intact rock subjected to cyclic loading”, *Int. J. Rock Mech. Min. Sci.*, **85**, 27-32. <https://doi.org/10.1016/j.ijrmmms.2016.03.003>.
- Liu, X.S., Tan, Y.L., Ning, J.G., Lu, Y.W. and Gu, Q.H. (2018), “Mechanical properties and damage constitutive model of coal in coal-rock combined body”, *Int. J. Rock Mech. Min. Sci.*, **110**, 140-150. <https://doi.org/10.1016/j.ijrmmms.2018.07.020>.
- Lyu, X.Z., Zhao, Z.H., Wang, X.J. and Wang, W.M. (2019), “Study on the permeability of weakly cemented sandstones”, *Geofluids*, <https://doi.org/10.1155/2019/8310128>.
- Ma, Q., Tan, Y.L., Zhao, Z.H., Xu, Q., Wang, J. and Ding, K. (2018), “Roadside support schemes numerical simulation and field monitoring of gob-side entry retaining in soft floor and hard roof”, *Arab. J. Geosci.*, **11**, 563. <https://doi.org/10.1007/s12517-018-3904-9>.
- Ma, S., Nemcik, J. and Aziz, N. (2014), “Simulation of fully grouted rockbolts in underground roadways using FLAC2D”, *Can. Geotech. J.*, **51**(8), 911-920. <https://doi.org/10.1139/cgj-2013-0338>.
- Mazaira, M.A. and Konicek, P. (2015), “Intense rockburst impacts in deep underground construction and their prevention”, *Can. Geotech. J.*, **52**(10), 1426-1439. <https://doi.org/10.1139/cgj-2014-0359>.
- Ning, J.G., Liu, X.S., Tan, J., Gu, Q.H., Tan, Y.L. and Wang, J. (2018), “Control mechanisms and design for a ‘coal-backfill-gangue’ support system for coal mine gob-side entry retaining”, *Int. J. Oil Gas Coal T.*, **18**(3-4), 444-465.
- Ning, J.G., Wang, J., Liu, X.S., Qian, K. and Sun, B. (2014), “Soft-strong supporting mechanism of gob-side entry retaining in deep coal seams threatened by rockburst”, *Int. J. Min. Sci. Technol.*, **24**(6), 805-810. <https://doi.org/10.1016/j.ijmst.2014.10.012>.
- Pappas, D.M. and Mark, C. (1993), “Behavior of simulated longwall gob material”, Report of Investigations, US Bureau of Mines.
- Pappas, D.M. and Mark, C. (1993), “Behavior of simulated longwall gob material”, Report of Investigation, Bureau of Mines, RI-9458, US Department of the Interior.
- Paul, A., Singh, A.P., John, L.P., Ajoy, K.S. and Manoj, K. (2012), “Validation of RMR-based support design using roof bolts by numerical modeling for underground coal mine of Monnet Ispat, Raigarh, India-a case study”, *Arab. J. Geosci.*, **5**(6), 1435-1448. <https://doi.org/10.1007/s12517-011-0313-8>.
- Qi, C.C., Chen, Q.S., Fourie, A. and Zhang, Q.L. (2018), “An intelligent modelling framework for mechanical properties of cemented paste backfill”, *Miner. Eng.*, **123**(16), 16-27. <https://doi.org/10.1016/j.mineng.2018.04.010>.
- Recio-Gordo, D. and Jimenez, R. (2012), “A probabilistic extension to the empirical ALPS and ARMPS systems for coal pillar design”, *Int. J. Rock Mech. Min. Sci.*, **52**, 181-187. <http://dx.doi.org/10.1016%2Fj.ijrmmms.2012.03.009>.
- Schumacher, F.P. and Kim, E. (2014), “Evaluation of directional drilling implication of double layered pipe umbrella system for the coal mine roof support with composite material and beam element methods using FLAC3D”, *J. Min. Sci.*, **50**(2), 335-348. <https://doi.org/10.1134/S1062739114020173>.
- Shi, G.Y. (2014), “Gateway retained along goaf technology with pier pillar backfilled with high water material in high gassy mine”, *Coal Sci. Tech.*, **42**(7), 30-32.
- Song, Z.Q., Cui, Z.D., Xia, H.C., Tang, J.C. and Wen, Z.J. (2010), “The fundamental theoretical on the green safe no coal pillar mining model by mainly using coal gangue backfill”, *J. Chin. Coal Soc.*, **35**(5), 705-710.
- Tan, Y.L., Gu, Q.H., Ning, J.G., Liu, X.S., Jia, Z.C. and Huang, D.M. (2019), “Uniaxial compression behavior of cement mortar and its damage-constitutive model based on energy theory”, *Materials*, **12**(8), 1309. <https://doi.org/10.3390/ma12081309>.
- Tan, Y.L., Yu, F.H., Ning, J.G. and Zhao, T.B. (2015), “Design and construction of entry retaining support along a gob-side under hard roof stratum”, *Int. J. Rock Mech. Min. Sci.*, **77**, 115-121. <http://dx.doi.org/10.1016%2Fj.ijrmmms.2015.03.025>.
- Thompson, B.D., Bawden, W.F. and Grabinsky, M.W. (2012), “In situ measurements of cemented paste backfill at the Cayeli Mine”, *Can. Geotech. J.*, **49**(7), 755-772. <https://doi.org/10.1139/t2012-040>.
- Wang, J., Ning, J.G., Jiang, J.Q. and Bu, T.T. (2018), “Structural characteristics of strata overlying of a fully mechanized longwall face: A case study”, *J. South Afr. Inst. Min. Metall.*, **118**(11), 1195-1204. <http://dx.doi.org/10.17159/2411-9717/2018/v118n11a10>.
- Wang, Y., Fall, M. and Wu, A. (2016), “Initial temperature-dependence of strength development and self-desiccation in cemented paste backfill that contains sodium silicate”, *Cement Concrete Compos.*, **67**, 101-110.
- Yang, H.Y., Cao, S.G., Wang, S.Q., Fan, Y.C., Wang, S. and Chen, X.Z. (2016), “Adaptation assessment of gob-side entry retaining based on geological factors”, *Eng. Geol.*, **209**, 143-151. <https://doi.org/10.1016/j.enggeo.2016.05.016>.
- Yang, X.K., Xiong, R., Yang, F., Yin, H.Q. and Yang, T. (2015), “Laboratory investigation of the high temperature rheological property of activated coal gangue modified asphalt binder”, *Appl. Mech. Mater.*, **744-746**, 1261-1265.
- Yin, D.W., Chen, S.J., Liu, X.Q. and Ma, H.F. (2018), “Effect of joint angle in coal on failure mechanical behavior of roof rock-coal combined body”, *Quart. J. Eng. Geol. Hydrogeol.*, **51**(2), 202-209. <https://doi.org/10.1144/qjegh2017-041>.
- Zhao, Z.H., Ma, Q., Chen, S.J., Ma, H. and Gao, X.J. (2018), “Prediction model of failure zone in roadway sidewall considering the lithologic effect of rock formation”, *Math. Prob. Eng.*, <https://doi.org/10.1155/2018/9627564>.
- Zhao, Z.H., Ma, Q., Tan, Y.L. and Gao, X.J. (2018), “Load transfer mechanism and reinforcement effect of segmentally yieldable anchorage in weakly consolidated soft rock”, *Simulation*, **95**(1), 83-96. <https://doi.org/10.1177%2F0037549718770284>.